EPJ Web of Conferences **319**, 05001 (2025) https://doi.org/10.1051/epjconf/202531905001
RICAP-24

Exploring NGC 3603 non-thermal emission through a realistic modelling of its environment

Manuel Rocamora[1,*], *Anita* Reimer[1], *Guillem* Martí-Devesa[2,3], and *Ralf* Kissmann[1]

[1]Universität Innsbruck, Institut für Astro- und Teilchenphysik, Technikerstr. 25/8, 6020 Innsbruck, Austria

[2]Dipartimento di Fisica, Universitá di Trieste, I-34127 Trieste, Italy

[3]Istituto Nazionale di Fisica Nucleare, Sezione di Trieste, 34127 Trieste, Italy

Abstract. We study the young and compact star-forming region NGC 3603, a well known γ-ray emitter. We build a novel non-thermal emission model by creating realistic 3D distributions of the gas and the radiation field in the region. We introduce these models into PICARD to perform cosmic-ray transport simulations and produce emission maps. The results are compared with a dedicated *Fermi* Large Area Telescope data analysis at high energies and with ATCA radio data. We improve the existing upper limits of the NGC 3603 γ-ray source extension. Although the γ-ray spectrum is well reproduced with the injection of CR protons, the resulting extension of the simulated hadronic source is in mild tension with the data upper limit. The radio data disfavours the lepton-only scenario. Combining both cosmic-ray populations the results are consistent with all observables.

1 Introduction

The number of detected Star-Forming Regions in the γ-ray band is rising, increasing the interest in understanding the acceleration mechanisms that might be playing a role in there. These regions typically contain many massive stars, which lose material through powerful winds and form a cavity in their surrounding medium [1]. In this cavity, also known as bubble, the collective winds of the stars develop a termination shock where particles can be accelerated through diffusive shock acceleration [DSA; 2]. It is not clear whether their cosmic-ray content is dominantly hadronic or leptonic: There have been many studies regarding the acceleration of particles in these systems where the leptonic component is, in general, not considered. However, the recent Westerlund 1 measurements by H.E.S.S. seem to be better explained using a leptonic scenario [3] for the γ-ray origin.

In this work, we explore the non-thermal properties of NGC 3603, a young and dense star-forming region. This system has been deeply studied over the whole electromagnetic spectrum and its physical characteristics are well determined. Furthermore, a γ-ray source in the direction of NGC 3603 was already detected [4], but the particle population underlying this emission remains unclear. We aim to probe the possibility of the γ-ray emission from NGC 3603 being produced by cosmic-ray electrons accelerated by the star cluster.

*e-mail: manuel.rocamora@uibk.ac.at

2 Method

We make use of the PICARD code [5], a cosmic-ray propagation solver, to study this γ-ray source. We build realistic 3D distributions of the gas density and radiation fields based on observations and introduce them into PICARD to perform dedicated cosmic-ray propagation simulations.

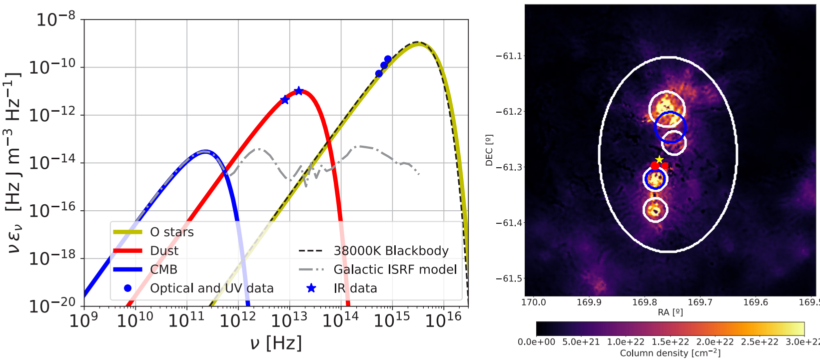

Figure 1. *Left:* Radiation density at the center of the Star-Forming region. Blue shows the CMB contribution, red shows dust and yellow shows stars. *Right:* H_2 column density. White lines show H_2 clouds, blue HI and red HII.

To build the target radiation field for particle-photon interactions, we extract the information from a catalogue of OB stars in the region [6]. In addition, we add the contributions from dust and the Cosmic Microwave Background (CMB). We refer to [7] for more details. The resulting radiation density in the center of the Star Cluster is shown in the left panel of Figure 1. We introduce H_2, HI and HII gas components in form of constant density clouds based on Herschel [8], 21 cm [9] and MUSE [10] data, respectively. The clouds are shown in white (H_2), blue (HI) and red (HII) contours in the right panel of Figure 1, respectively.

2.1 Particle injection and propagation

We assume the acceleration mechanism in NGC 3603 to be DSA at the termination shock of the collective wind and consider three different scenarios: a purely leptonic case; a purely hadronic scenario; and, finally, a hybrid setup, where both electrons and protons are injected. Additionally, secondary electrons and positrons will be produced through pp-interactions in the scenarios containing CR protons. The energy injected into the cosmic rays is limited by the kinetic wind luminosity.

After being injected, the particles propagate and suffer further energy gains and losses. The Kolmogorov regime is assumed for the diffusion of the particles [1], leading to a diffusion coefficient of $D(E) = 4.0 \cdot 10^{26}$ cm^2/s [2]. A radial collective wind of $v_W = 2500$ km/s is assumed to account for convection. Finally, we consider a constant magnetic field of 7 μG, based on MHD simulations [11].

3 Gamma-ray Observations

We perform a morphological and spectroscopic analysis of NGC 3603 in the GeV photon band. We make use of more than 15 years of LAT data, selecting P8R3 `SOURCE` data (evclass = 128) between 1 GeV and 1 TeV, with a cut on the zenith angle $z_{\max}$ at 105°. This description provides an optimal ROI background at energies where LAT performs best, yet it is insufficient to achieve either the spectral or morphological objectives of the present analysis. To this end we employ two additional analyses: setting the low energy thresholds at 100 MeV and 10 GeV, respectively. We refer again to [7] for more information about the analyses. The latter analysis, optimal for the morphological determination, provides an upper limit of 0.096° on the extension of the γ-ray source, improving the 0.12° from the previous analysis [4].

4 Results

It is mainly the γ-ray spectrum that is used to constrain the free parameters in our model. We test several injection indices and choose the one resulting in the best chi-square.

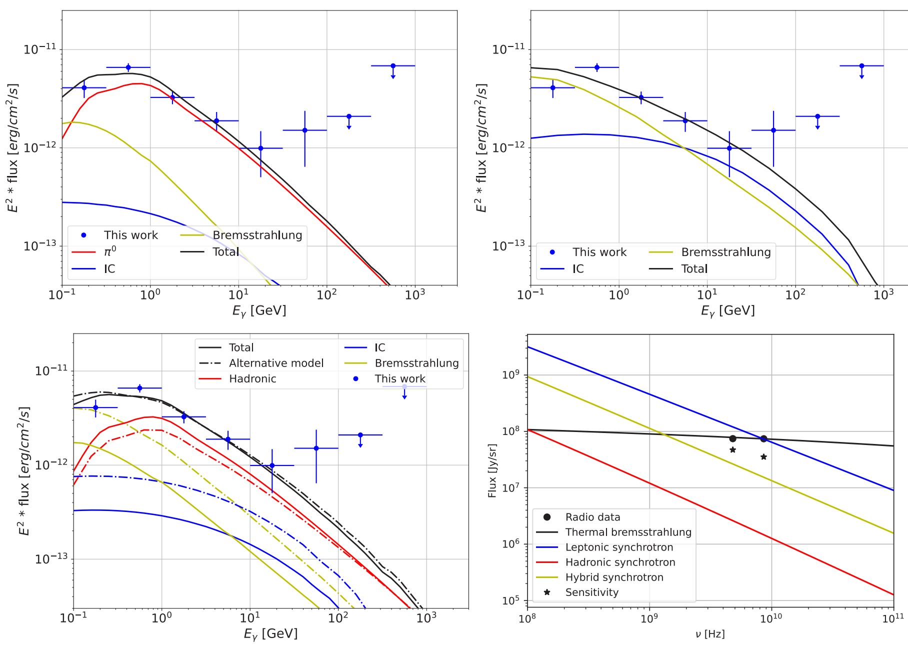

Figure 2. *Upper left:* Hadronic γ-ray spectrum. *Upper right:* Leptonic γ-ray spectrum. *Lower left:* Hybrid γ-ray spectrum. *Lower right:* Radio spectrum.

The chi-square fit results in an injection index of $\alpha_{had} = 2.6$ and an acceleration efficiency near to 30% for protons-only injection model. The final γ-ray spectrum is shown in the upper left panel of Figure 2. The extension of the simulated hadronic γ-ray source is 0.098°, in mild tension with the data upper limit. In the leptonic-only scenario, in the upper right panel, the γ-ray fit is worse. The final injection index is $\alpha_{lep} = 2.5$ and the acceleration efficiency is 0.4%. However, the extension of the γ-ray source is 0.086°, consistent with the data upper limit. When injecting both types of particles, the best-fit leads to $\alpha_{hyb,p} = 2.55$, $\alpha_{hyb,e} = 2.65$, an efficiency of around 20% and a p/e ratio of 200. The spectrum is represented as solid lines in the lower left panel of Figure 2 and the γ-ray extension in this case is 0.096°. Nevertheless, we show that this extension can be reduced with still a decent fit of the spectrum. This modified model is represented as dash-dotted lines, using a p/e ratio of 80 and an efficiency of 10%, with an extension of 0.093°.

Cosmic-ray leptons emit in the radio band through synchrotron radiation. Our simulated source is much more extended than the one observed by ATCA [12], which is quasi-point-like at wavelengths of 3 and 6 cm. With this incompatibility in size, our results should be below the sensitivity of the instrument, shown as black stars in the lower right panel of Figure 2, in order to be compatible. This results disfavour the lepton-only scenario.

5 Discussion & Conclusions

Our approach to model the extension in the hadronic scenario is robust, since it does not depend on the propagation setup. Due to the small size of the region, even when reducing the diffusion coefficient, the particles are able to reach the locations where the γ rays are produced. Therefore, the results are mainly determined by the angular size of the observations.

Coming back to the main question of this work, the pure hadronic scenario presents a light tension with the data upper limit on the extension of the γ-ray source. Although this tension is only mild considering the analysis uncertainties, it can be avoided by introducing primary electrons. Primary electrons on their own also have difficulties explaining the multiwavelength data due to conflicts with the radio observations. Therefore, the high-energy emission from NGC 3603 more likely originates from a mixture of cosmic-ray electrons and protons.

References

[1] Gallegos, M., et al., Winds in Star Clusters Drive Kolmogorov Turbulence. ApJ **899**, L30 (2020) https://doi.org/10.3847/2041-8213/ababae

[2] Morlino, G., et al., Particle acceleration in winds of star clusters. MNRAS **504**, 6096 (2021) https://doi.org/10.1093/mnras/stab690

[3] Härer, L., et al., Understanding the TeV γ-ray emission surrounding the young massive star cluster Westerlund 1. A&A **671**, A4 (2023) https://doi.org/10.1051/0004-6361/202245444

[4] Saha, L., et al., Morphological and Spectral Study of 4FGL J1115.1-6118 in the Region of the Young Massive Stellar Cluster NGC 3603. ApJ **897**, 131 (2020) https://doi.org/10.3847/1538-4357/ab9ac2

[5] Kissmann, R., PICARD: A novel code for the Galactic Cosmic Ray propagation problem. Astroparticle Physics **55**, 37 (2014) https://doi.org/10.1016/j.astropartphys.2014.02.002

[6] Drew, J. E., et al., The O star hinterland of the Galactic starburst, NGC 3603. MNRAS **486**, 1034 (2019) https://doi.org/10.1093/mnras/stz864

[7] Rocamora, M, et al., Exploring non-thermal emission from the star-forming region NGC 3603 through a realistic modelling of its environment. Arxiv (2024) https://doi.org/10.48550/arXiv.2411.05206

[8] Schneider, N., et al., Understanding star formation in molecular clouds. I. Effects of line-of-sight contamination on the column density structure. A&A **575**, A79 (2015) https://doi.org/10.1051/0004-6361/20142356

[9] Retallack, D. S. et al., High-resolution radio observations of three southern H II regions. MNRAS **193**, 261 (1980) https://doi.org/10.1093/mnras/193.2.261

[10] McLeod, A. F., et al., Connecting the dots: a correlation between ionizing radiation and cloud mass-loss rate traced by optical integral field spectroscopy. MNRAS **462**, 3537 (2016) https://doi.org/10.1093/mnras/stw1864

[11] Badmaev, D. V., et al., Inside the core of a young massive star cluster: 3D MHD simulations. MNRAS **512**, 2818 (2022) https://doi.org/10.1093/mnras/stac2738

[12] Mücke, A., et al., Australia Telescope Compact Array Radio Imaging of the Proplyd-like Objects in the Giant H II Region NGC 3603. ApJ **571**, 366 (2002) https://doi.org/10.1086/339843